Hindawi
Mathematical Problems in Engineering
Volume 2017, Article ID 8325040, 14 pages
https://doi.org/10.1155/2017/8325040

Research Article

Off-Design Behavior Analysis and Operating Curve Design of Marine Intercooled Gas Turbine

Nian-kun Ji, Shu-ying Li, Zhi-tao Wang, and Ning-bo Zhao

College of Power and Energy Engineering, Harbin Engineering University, Harbin 150001, China

Correspondence should be addressed to Zhi-tao Wang; wangzhitao@hrbeu.edu.cn

Received 16 January 2017; Revised 13 April 2017; Accepted 30 April 2017; Published 5 June 2017

Academic Editor: Marco Pizzarelli

The intercooled gas turbine obtained by adopting an indirect heat exchanger into an existing gas turbine is one of the candidates for developing high-power marine power units. To simplify such a strong coupled nonlinear system reasonably, the feasibility and availability of qualifying equivalent effectiveness as the only parameter to evaluate the intercooler behavior are investigated. Regarding equivalent effectiveness as an additional degree of freedom, the steady state model of a marine intercooled gas turbine is developed and its off-design performance is analyzed. With comprehensive considerations given to various phase missions of ships, operational flexibility, mechanical constraints, and thermal constraints, the operating curve of the intercooled gas turbine is optimized based on graphical method in three-dimensional performance space. The resulting operating curve revealed that the control strategy at the steady state conditions for the intercooled gas turbine should be variable cycle control. The necessity of integration optimization design for gas turbine and intercooler is indicated and the modeling and analysis method developed in this paper should be beneficial to it.

1. Introduction

Continuous improvement of gas turbines performance is an eternal topic. For conventional gas turbines, this can be achieved mainly by increasing overall pressure ratio (OPR) and turbine inlet temperature (TIT). However, the level of OPR and TIT depends on future advancements in material and cooling technology [1, 2]. Complex cycle provides another approach for improving performance of gas turbines. Intercooling reconstruction based on existing gas turbines has been demonstrated as a practicable method for developing complex cycle [3, 4].

An intercooler with minimum size, lowest pressure losses, and maximum effectiveness should be suggested for enhancing the performance of an intercooled gas turbine. As these requirements tend to conflict with each other, the optimization of an intercooler becomes more important. Xiao [5] studied a multiobjective model and then selected an improved Alopex algorithm in the work of intercooler optimization. Dong et al. [6] designed and optimized a modularized intercooler for marine gas turbine. Optimization and assessment of a cross-flow heat exchanger for advanced intercooled cycle aero engines were carried out using CFD method by Kim et al. [7]. The correlation between heat transfer and loss characteristics has been emphasized during conceptual design of a two-pass cross-flow aeroengine intercooler [8]. Zhao et al. [9] studied the effects of different materials and different coolants on intercooler performance and developed intercooler optimization by using simulated annealing algorithm. We found that, in previous research activities for intercooler optimization, inlet parameters of the cold side were often assumed as a constant or a range. And inlet parameters of hot side were often estimated by the operation conditions of the existing gas turbines. In practice the variation of inlet parameters makes the optimization of intercoolers more complicated. Even though the off-design behavior of an existing gas turbine was fully considered, we could not ensure the optimized intercooler optimal because intercooling will make the working points jump from the existing (original) gas turbine to the intercooled (new) gas turbine.

On the other hand, satisfactory performance design of an intercooled gas turbine at steady state conditions depends on off-design behavior investigations. There are many previous

studies about gas turbine optimization. Some guiding principles for assessing part-load performance of different gas turbine schemes have been indicated by Mallinson and Lewis [10] as early as 1948. Methods and conclusions in this literature offer insight into studies of intercooled cycle, although some approximations have been made; for example, pressure loss in the intercooler was assumed to be small percentage of the entry pressure, and temperature after intercooler was regarded as constant. da Cunha Alves et al. [11] found that the efficiency advantages of the intercooled cycles appeared at high OPR, and the intercooler location was suggested to be after the early stages of the compressor, by comparing intercooled cycle with other cycles. Wang et al. [12] obtained thrice-maximum power of an irreversible closed intercooled regenerated Brayton cycle based on considering various losses in heat exchangers and treating some original design parameters such as intercooler effectiveness and seawater outlet temperature as constant. Chen et al. [13–16] studied a modeling approach for a triple-shaft open ICR gas turbine and obtained analytical formulas of the cycle's performance with 19 pressure drop losses, as well as optimizing the performance of the model cycle, reaching some valuable conclusions. Canière et al. [17] studied the influence of various outlet pressure and temperature of intercooler and consequent various cooling air parameters on the gas turbine. Many of the aforementioned studies that carried out the effect of intercooler on gas turbine performance nevertheless did not value the effect of gas turbine performance back on intercooler enough.

So it is necessary to consider the intercooler and the gas turbine simultaneously, not only in intercooler optimization but also in gas turbine optimization. Researchers clarified the importance of coupling of intercoolers and gas turbines recently, mainly in aeroengine field [18–20].

In the work presented here, a coupling model of a marine intercooled gas turbine is established for off-design behavior analysis. Based on optimizing operating curve in three-dimensional performance space, subsection control is deduced for the marine intercooled gas turbine at the steady state.

2. Description of Research Object

The schematic layout of an typical intercooled gas turbine for marine application is shown in Figure 1 with station numbers definition. The main features of the intercooled gas turbine in this study are summarized below:

(1) The intercooled gas turbine is developed from an existing dual-shaft gas generator with a power turbine, only by inserting an intercooler between the low pressure compressor (LPC) and high pressure compressor (HPC). Although the redesigning of some components (compressor and turbine stages, combustion chamber, etc.) can improve the performance of intercooled gas turbine [3, 4], the minimum conversion here has many advantages such as inheriting the reliability of the prototype, reducing design and development cost, and using all component characteristic maps available. The increase of the low pressure shaft dimension and corresponding deteriorative mechanical performance is ignored here.

(2) The indirect fluid coupling intercooler is composed of two parts, that is, the on-engine intercooler and the off-engine intercooler. This kind of configuration is mainly based on the consideration of assembly space, corrosion resistance, and maintainability. Through the medium of ethylene glycol (EG) solution with 50% volume fraction, a part of heat in compressed air at LPC outlet transfers to seawater in two steps. Consequently output power of the intercooled gas turbine increases because of less work required for HPC.

(3) The negative effects of intercooling have been reported in previous studies [11, 18, 20–23], but the power consumption of pumps to drive intercoolers has received limited attention. One way to reflect the drawback of the intercooling better is regarding the pumps as customers of the output power offered by the intercooled gas turbine. But this will strengthen the coupling among gas turbine, on-engine intercooler, and off-engine intercooler, which makes the task of modeling and analyzing more challenging.

3. Off-Design Behavior Model

In order to ensure the trade-off between validity and complexity of the off-design behavior model, some necessary assumptions are made as follows:

(1) For highlighting the interaction between the intercooler and the existing gas turbine in the strongly coupled system, the operation environment will be restricted to sea-level in a standard atmosphere at temperature of 273.15 K (15°C) and pressure of 101.325 kPa (1 atm).

(2) For simplifying the coupling between the on-engine intercooler and the off-engine intercooler moderately, we assume the complex process of heat exchange between ambient air and seawater performed thoroughly and the air/sea temperature difference will be ignored. In fact the air/sea temperature difference generally varies near the zero under the influence of many factors [24–26].

(3) The condensation of moist air will be ignored with regard to the working fluid on the air side as ideal gas.

3.1. Definition of Equivalent Effectiveness. The information flow in the model of the intercooled gas turbine is illustrated in Figure 2. The coupling between the two heat exchangers is mainly reflected in that the coolant of EG solution acts as cooling fluid in on-engine intercooler and as the heating fluid in off-engine intercooler simultaneously. So the temperature of EG flowing into the on-engine intercooler ($T_{\mathrm{EG.in.on}}$) equals the temperature of EG flowing out of the off-engine intercooler ($T_{\mathrm{EG.out.off}}$), and similarly the inlet temperature

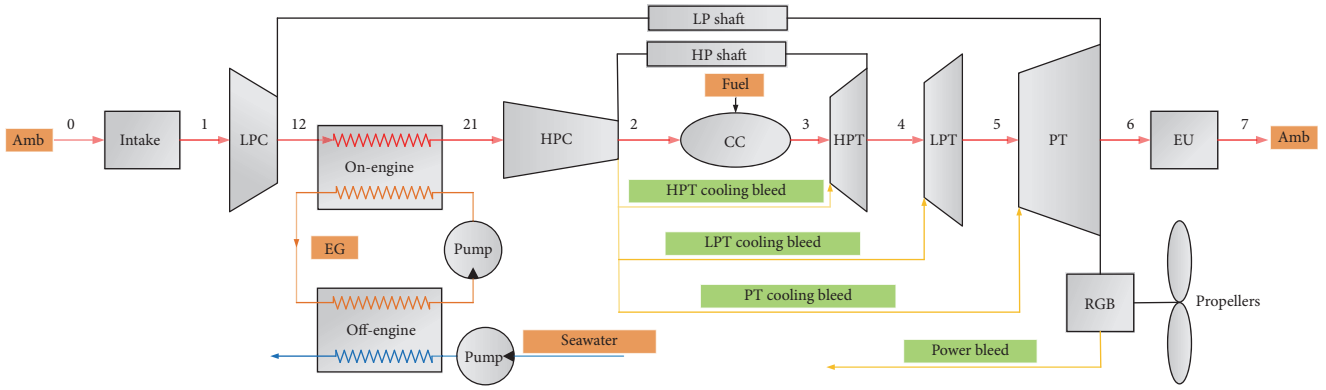

Figure 1: Schematic layout of intercooled gas turbine for marine application.

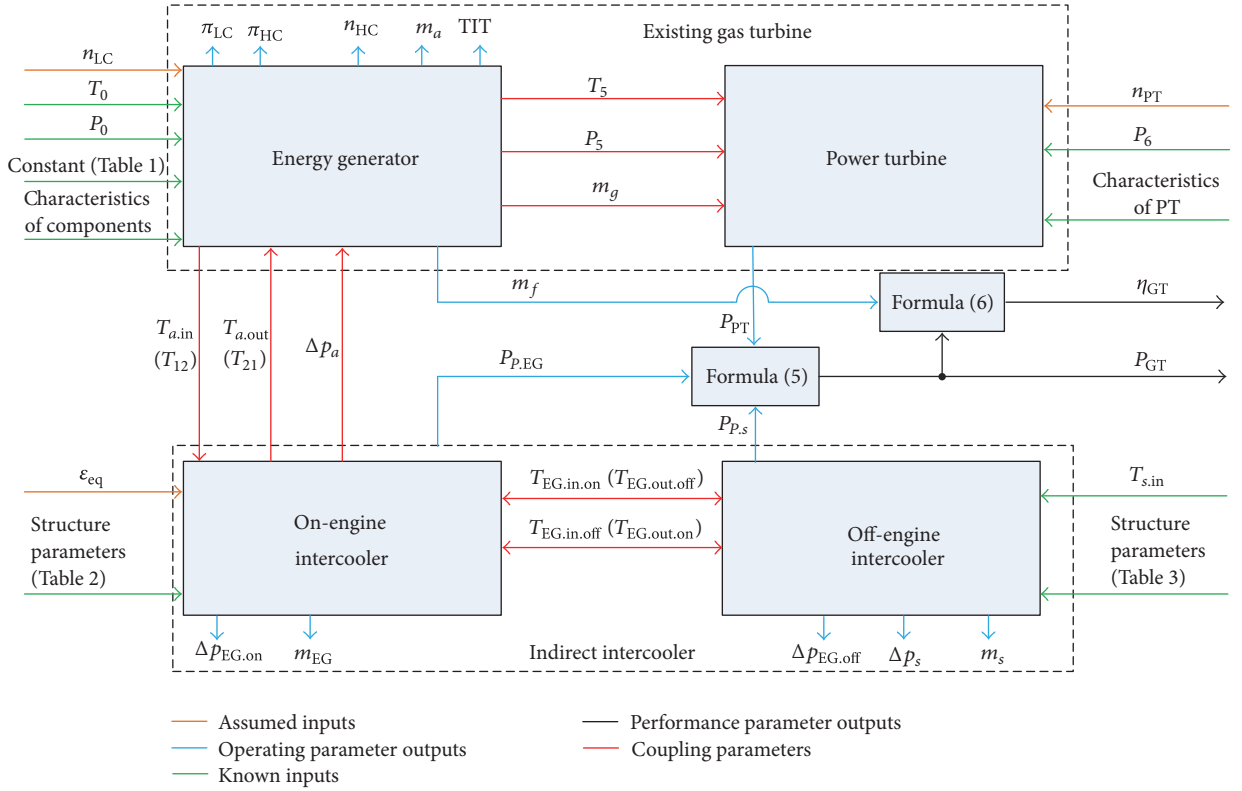

Figure 2: Information flow in the model of intercooled gas turbine.

of EG in off-engine intercooler ($T_{EG.in.off}$) equals the outlet temperature of EG in on-engine intercooler ($T_{EG.out.on}$).

In order to provide a reduced order model suitable for the intercooled gas turbine, the two heat exchangers are regarded as one. Imitating the forms of effectiveness of ordinary heat exchangers, a nondimensional parameter named equivalent effectiveness (ε_{eq}) is defined for the indirect fluid coupling intercooler as

$$\varepsilon_{eq} = \frac{T_{a.in} - T_{a.out}}{T_{a.in} - T_{s.in}}, \quad (1)$$

where $T_{a.in}$, $T_{a.out}$, and $T_{s.in}$ are inlet temperature of compressed air, outlet temperature of compressed air, and inlet temperature of seawater, respectively.

With LPC working at a certain operating condition, $T_{a.in}$ (equal to the outlet temperature of LPC, T_{12}) can be determined. Based on the second assumption above (i.e., $T_{s.in}$ equals the intake temperature of the gas turbine), formula (1) shows that $T_{a.out}$ (equal to the inlet temperature of HPC, T_{21}) is correlative only with ε_{eq}.

Once $T_{a.in}$ and $T_{a.out}$ are known, the pressure drop of the air flow (ΔP_a) in the intercooler can be determined using an iterative algorithm. The concrete implementation steps about such an iterative algorithm are listed below.

Step 1. Suppose $\Delta P_a'$ as the initial value of the pressure drop and calculate corresponding outlet pressure (P_{21}) of the air flow in the intercooler.

Step 2. Determine the inlet specific volume (υ_{in}) of the air flow by $T_{a.\text{in}}$ and P_{12}. Determine the outlet specific volume (υ_{out}) of the air flow by $T_{a.\text{out}}$ and P_{21}.

Step 3. Calculate the total pressure drop (ΔP_a) using the parameters of the air flow in the intercooler. Considering the pressure drop of inlet channels (ΔP_{in}), the pressure drop of core part (ΔP_{core}), and the pressure drop of outlet channels (ΔP_{out}), the total pressure drop (ΔP_a) in the intercooler can be formulated [27] as

$$\begin{aligned}
\Delta P_a &= \Delta P_{\text{in}} + \Delta P_{\text{core}} + \Delta P_{\text{out}} \\
\Delta P_{\text{in}} &= \frac{g_m^2 \upsilon_{\text{in}}}{2}\left(1 - \alpha^2 + K_{\text{in}}\right) \\
\Delta P_{\text{core}} &= \frac{g_m^2 \upsilon_{\text{in}}}{2}\left[2\left(\frac{\upsilon_{\text{out}}}{\upsilon_{\text{in}}} - 1\right) + \frac{4fL_1}{d_e}\cdot\frac{\upsilon_m}{\upsilon_{\text{in}}}\right] \\
\Delta P_{\text{out}} &= \frac{g_m^2 \upsilon_{\text{out}}}{2}\left(1 - \alpha^2 - K_{\text{out}}\right),
\end{aligned} \tag{2}$$

where g_m is the mass flow rate of air, which can be determined by the ratio of air flow to the minimum value of the free flow area. υ_m is the mean specific volume along the component length and can be obtained approximately by average value of υ_{in} and υ_{out}. L_1, d_e, and α are structure parameters of heat exchanger, representing length, hydraulic diameter, and the ratio of channel free flow area to cross-sectional area, respectively. K_{in}, K_{out}, and f are the pressure loss coefficient of inlet, the pressure loss coefficient of outlet, and the fanning friction factor of the core part, respectively. These three empirical coefficients are all related not only to Reynolds number but also to channel geometries.

Step 4. Compare ΔP_a with $\Delta P_a'$. If the difference value of them can meet the precision requirement, stop the iteration. Otherwise, come back to Step 1.

Therefore, ε_{eq} can be qualified to act as the only parameter representing the effect of the indirect intercooler to the existing gas turbine in the off-design condition of the intercooled gas turbine.

3.2. Off-Design Performance Computation. On account of the direct influence of the intercooler to HPC, low pressure rotor speed (n_{LC}) is selected as an independent parameter of the intercooled gas turbine. Another two independent parameters are ε_{eq} and the power turbine speed (n_{PT}); namely, the intercooled gas turbine has three degrees of freedom. Accordingly, it can be seen in Figure 2 that n_{LC}, ε_{eq}, and n_{PT} act as assumed input variables in the off-design behavior model. In this section, a "decoupling-coupling" scheme is designed for the numerical simulations for off-design performance of intercooled gas turbine. The calculation flow chart is shown in Figure 3.

Firstly, in decoupling, since ε_{eq} was qualified to be the only parameter to represent the effect of the indirect intercooler to the existing gas turbine, the coupling between the two parts weakened. Therefore once the free parameters (n_{LC}, n_{PT}, and ε_{eq}) are assumed, the numerical simulations for off-design performance of intercooled gas turbine can be divided into two calculations performed simultaneously. One is the thermodynamic calculation for the gas turbine on account of additional temperature drop and pressure drop caused by the intercooler, which is aimed at searching for its matching operating points. Another is the thermodynamic calculation for the intercooler, which is aimed at searching for its matching operating parameters in the sense of minimum power consumption of pumps.

Secondly, in coupling, to avoid the negative effects of intercooling ignored, the power consumption of pumps to drive EG and seawater is taken into account. Therefore the final output power of the intercooled gas turbine will be expressed as the rest of the power of power turbine after deducting the power consumption of pumps.

As can be seen in the left dotted box of Figure 3, for the on-engine intercooler, with respect to a certain ε_{eq}, each set of the parameters of ε_{on} and ε_{off} can determine the inlet temperature and the outlet temperature of EG. For the off-engine intercooler, an iteration algorithm is required to estimate the outlet temperature of seawater ($T_{s.\text{out}}$), which is detailed as the following steps.

Step 1. Assume a value of $T_{s.\text{out}}$.

Step 2. Calculate the overall heat transfer coefficient by the basic equation of heat transfer in the off-engine intercooler and record it as K_{off}.

$$K_{\text{off}} = \frac{\Phi}{A \cdot \Delta t_m}, \tag{3}$$

where Φ is the amount of heat transfer from EG to seawater and A is the total heat transfer area of the off-engine intercooler. Determine the logarithmic mean temperature difference Δt_m which is the logarithmic mean temperature difference between EG and seawater which can be obtained by $T_{\text{EG.in.off}}$, $T_{\text{EG.out.off}}$, $T_{s.\text{in}}$, and $T_{s.\text{out}}$.

Step 3. Calculate the convective heat transfer coefficient of EG (α_{EG}) and seawater (α_s) by the heat transfer correlations of the off-engine intercooler. Taking no account of fouling thermal resistance, the overall heat transfer coefficient can be obtained and recorded as K_{off}'.

$$K_{\text{off}}' = \left(\frac{1}{\alpha_{\text{EG}}} + \frac{1}{\alpha_s}\right)^{-1}. \tag{4}$$

Step 4. Compare K_{off}' with K_{off}. If the difference value between them can meet the precision requirement, stop the iteration. Otherwise, come back to Step 1.

Hence all parameters about temperature of the off-engine intercooler have been known; the thermodynamic calculation for the indirect fluid coupling intercooler can be treated as the check of two heat exchangers on the basis of conservation law of energy and conservation law of mass. With respect to a certain ε_{eq}, each set of the parameters of ε_{on} and ε_{off} can determine a working condition of the

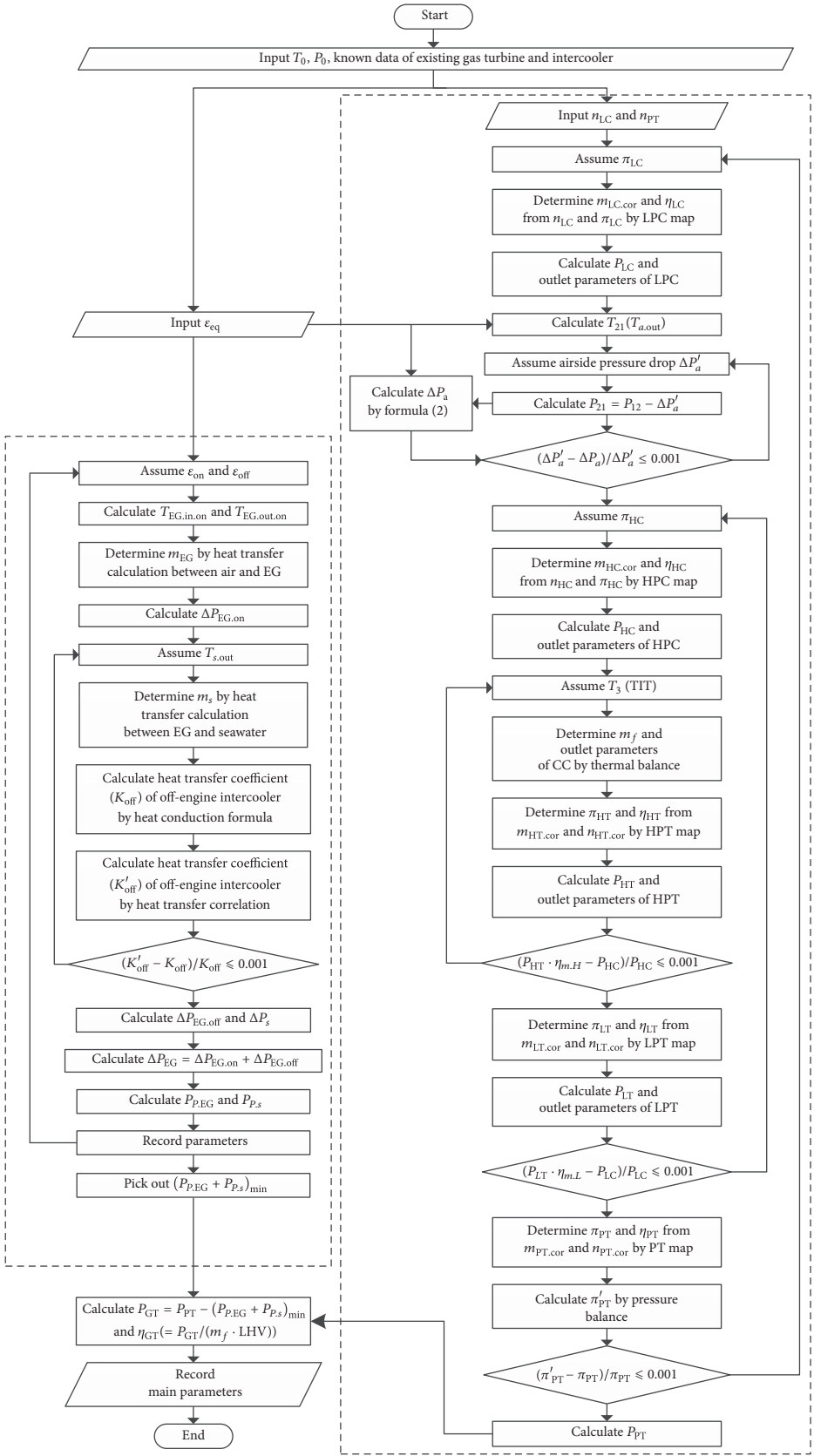

Figure 3: Calculation flow chart for off-design performance of intercooled gas turbine.

indirect fluid coupling intercooler. The pressure drop of air (ΔP_a) and the pressure drop of EG ($\Delta P_{\text{EG.on}}$) in the on-engine intercooler can be determined in the way of formula (2). The pressure drop of EG ($\Delta P_{\text{EG.off}}$) and the pressure drop of seawater (ΔP_s) in the off-engine intercooler can be determined by correlation formulas offered by its producer. The power consumption of pump to drive EG ($P_{P.\text{EG}}$) and power consumption of pump to drive seawater ($P_{P.s}$) can be obtained, too.

Changing the values of ε_{on} and ε_{off}, all of the behavior of the indirect fluid coupling intercooler can be obtained. It is not difficult to pick out the optimal working condition of the intercooler in the sense of the minimum power consumption of pumps expressed as $(P_{P.\text{EG}} + P_{P.s})_{\min}$.

As can be seen in the right dotted box of Figure 3, the thermodynamic calculation for the gas turbine on account of additional temperature drop and pressure drop caused by the intercooler has nearly the same rules as that for common gas turbines [28, 29]. The supplied fuel is assumed to completely combust in combustor and the back pressure on the power turbine is assumed to be fixed at ambient pressure. The matching requires satisfying various constraints such as rotational speed balance between turbines and compressors, power balance between turbines and compressors, thermal balance in combustion chamber, pressure balance, and continuity requirement along flow path. Once all these constraints are satisfied, the power generated by power turbine (P_{PT}) can be obtained, and many meaningful operating parameters can be recorded for analysis purposes, for example, high pressure rotor speed (n_{HC}), air mass flow rate (m_a), fuel mass flow rate (m_f), temperature, and pressure at various stations. By considering the minimum power consumption of pumps aforementioned, the output power and the thermal efficiency of the intercooled gas turbine are formulated as follows:

$$P_{\text{GT}} = P_{\text{PT}} - \left(P_{P.\text{EG}} + P_{P.s}\right)_{\min} \tag{5}$$

$$\eta_{\text{GT}} = \frac{P_{\text{GT}}}{m_f \cdot \text{LHV}}. \tag{6}$$

Accordingly, all of the behavior of the intercooled gas turbine can be obtained by changing values of the free parameters of n_{LC}, ε_{eq}, and n_{PT}.

In this model, component characteristics curves of existing gas turbine and structure parameters of intercooler are applied as known input data. Physical parameters such as specific heat capacity of air, gas, EG, and seawater are all regarded as functions of temperature and composition. A MATLAB code has been developed for realizing the off-design performance computation described by Figure 3.

3.3. Computation Example and Results. The gas turbine in the research literature [30] is applied to the existing gas turbine in this computation example with some parameters kept constant approximately, as shown in Table 1. A reverse flow plate-fin heat exchanger made of copper-nickel alloy has been optimized by Zhang [31]. In this study we choose it as the on-engine intercooler whose geometric structure is given in Table 2. A product (model BRS06) of Beijing Jinghai Heat Transfer Equipment Manufacturing Co., Ltd., acts as the off-engine intercooler [32]. This is a reverse flow plate heat exchanger and its structure parameters are listed in Table 3.

Table 1: Approximate values applied to inputs for computation.

Parameters	Values
Total pressure recovery coefficient of inlet (%)	96.8
Total pressure recovery coefficient of exhaust unit (%)	98.8
Mechanical efficiencies of low pressure shaft (%)	99
Mechanical efficiencies of high pressure shaft (%)	99
Bleed flows ratio for HPT cooling (%)	7.4
Bleed flows ratio for LPT cooling (%)	3.2
Bleed flows ratio for PT cooling (%)	2.6
Lower heating value of fuel (MJ/kg)	44.6

Table 2: Geometric structure of the on-engine intercooler.

Parameters	Values of the air side	Values of the coolant side
Number of fin layers	66	67
Plate pitch (mm)	6.0	2.0
Fin pitch (mm)	2.0	2.0
Plate thickness (mm)	0.3	0.3
Fin thickness (mm)	0.15	0.15
Seal thickness (mm)	6.0	6.0
Volume of intercooler (mm^3)	$435 \times 420 \times 400$	

Table 3: Geometric structure of the off-engine intercooler.

Parameters	Values
Plate area (m^2)	0.596
Plate thickness (mm)	0.8
Plate pitch (mm)	3.8

Table 4: Value space of free parameters.

Free parameters	Minimum values	Maximum values	Intervals
n_{LC} (r/min)	6000	7700	100
ε_{eq}	0	0.75	0.05
n_{PT} (r/min)	2400	3500	100

From the perspectives of mathematics, with an existing gas turbine, once the configuration of the intercooler is picked, almost each possible combination of the free parameters (n_{LC}, ε_{eq}, and n_{PT}) can result in a cooperating point of the intercooled gas turbine based on the model developed in Section 3.2, unless some parameters conflict with the constraints in physics (detailed analyses will be given in Section 4.2). The value ranges and intervals of the free parameters are listed in Table 4. Based on the known conditions given above, more than 3000 cooperating points are obtained by carrying out the off-design behavior model of the intercooled gas turbine. The corresponding operating parameters and performance parameters of these points are recorded for analysis.

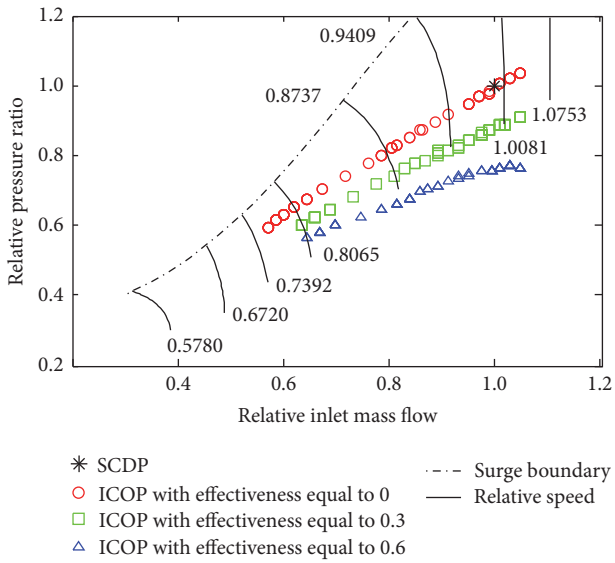

Figure 4: Operating points in LPC map.

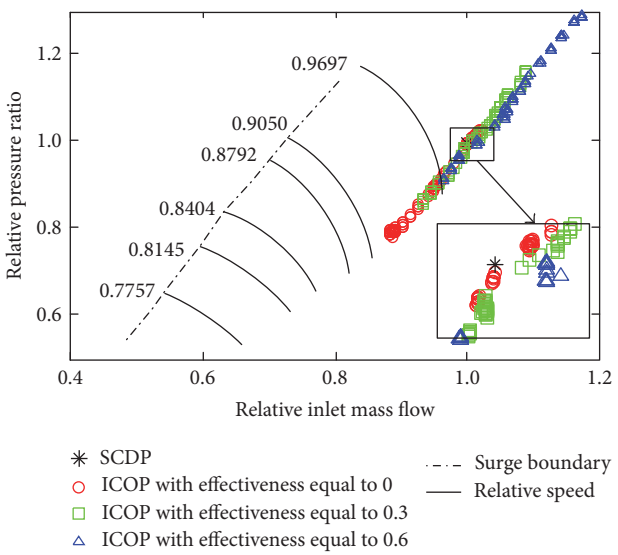

Figure 5: Operating points in HPC map.

4. Off-Design Performance Analysis and Operating Curve Design

The objective in the following section is to design an appropriate operating scheme for the intercooled gas turbine based on graphical method, with full considerations of requirements of different mission phase of ships, operational flexibility, and mechanical and thermal constraints of gas turbine components such as surging of compressors, overheating of turbines, and overspeeding of rotors. During this process the off-design behavior of the intercooled gas turbine is understood enough too.

4.1. Intercooling Effects on Surge Margin. As a kind of harmful abnormal condition of gas turbine, compressor surge presents the most impassable constraint and must be avoided anyhow. Fortunately, the operational range of intercooled gas turbine in this study cannot be restricted by the compressors' surge boundaries. Isolines of ε_{eq} at 0.3 intervals are illustrated in LPC map (Figure 4) and in HPC map (Figure 5), respectively. It can be observed in Figure 4 that the operating points with the same ε_{eq} value are almost in one line which moves away from the surge boundary when ε_{eq} increases; that is, the surge margin of LPC increases when ε_{eq} increases. In contrast the operating points move toward upper right almost along the same line with ε_{eq} increasing, as can be seen in Figure 5. On the basis of aforementioned reason, It is not necessary to mention the surge margin below as the constraint in the performance optimization of the intercooled gas turbine.

4.2. Operating Curve Design. By regarding the equivalent effectiveness as an additional degree of freedom, operation curve design of the intercooled gas turbine can be performed based on isosurfaces in a three-dimensional space with dimensionless coordinates of $\overline{n}_{PT}$, ε_{eq}, and $\overline{P}_{GT}$ (Figure 6). Here a parameter with a horizontal line on top expresses the ratio of the value at present (intercooled cycle) to the value at the design point of the existing gas turbine (simple cycle).

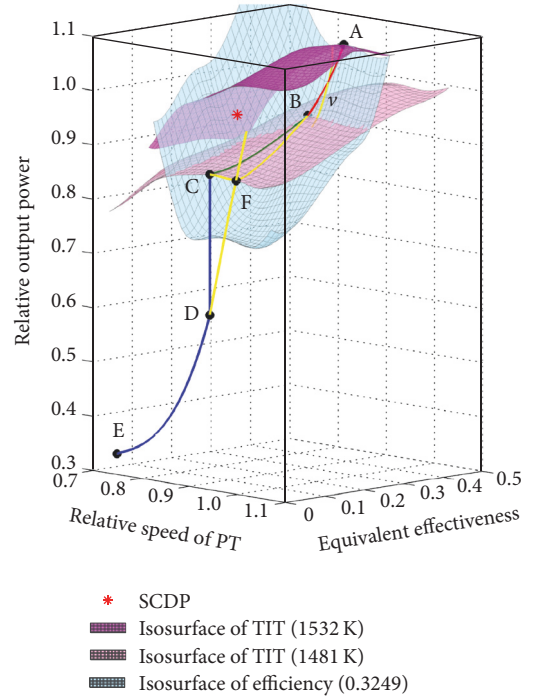

Figure 6: Operating curve design in three-dimensional performance space.

4.2.1. Maximum Power with Time Limit (Status A). The maximum power permits a ship to obtain maximum speed and excellent maneuverability within a short time, while components of gas turbine are mostly subject to hard operating conditions, among which HPT inlet temperature (TIT) has a crucial effect on gas turbine. In this case a TIT of 1532 K

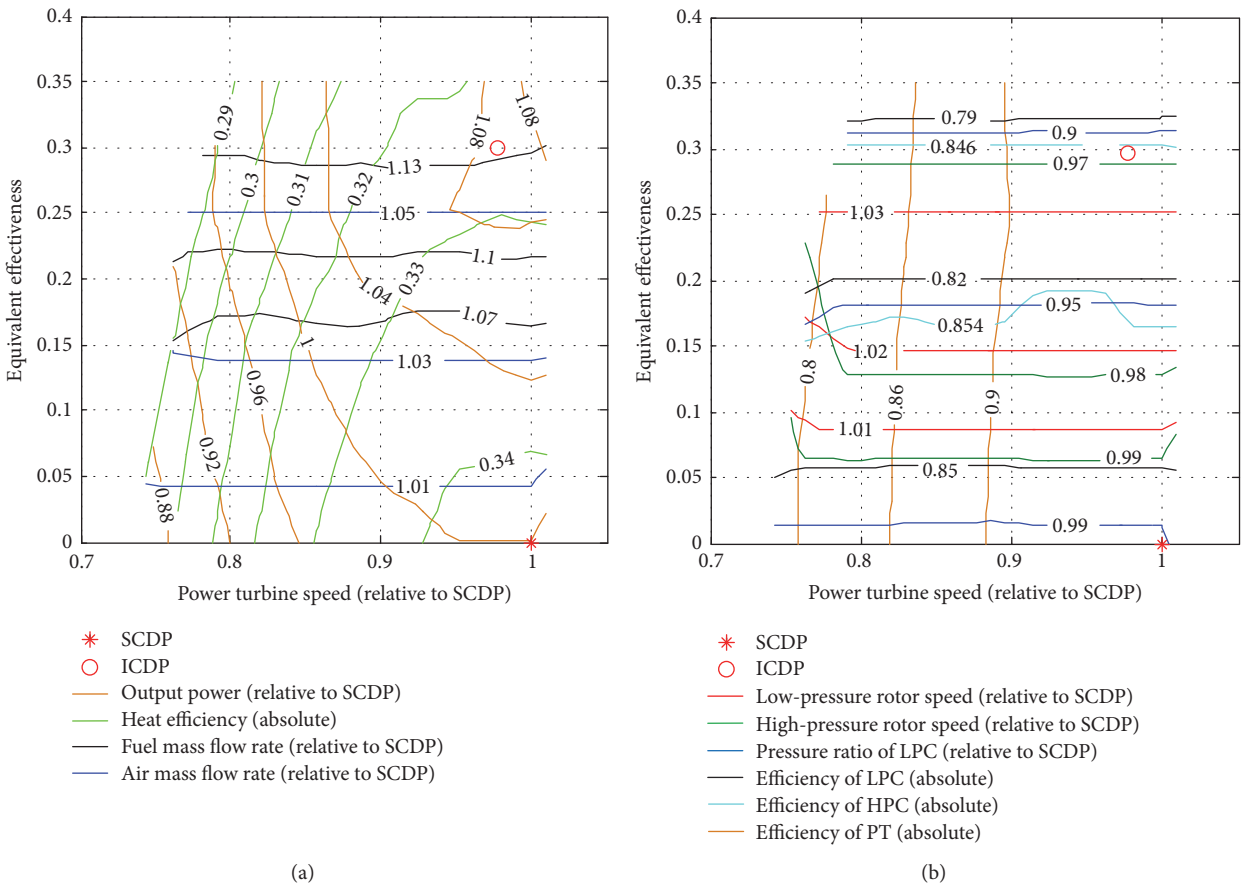

Figure 7: Meaningful parameters of intercooled gas turbine for TIT = 1532 K.

at the design point of the existing gas turbine is regarded as the upper limit of the TIT of the intercooled gas turbine. So the maximum power point of the intercooled gas turbine can be found at the peak of the isosurface of 1532 K, marked with letter A (0.9767, 0.2983, and 1.091) in Figure 6.

Figure 7 provides some meaningful parameters of the intercooled gas turbine with constant TIT of 1532 K in two-dimensional coordinate planes. The design point of the existing gas turbine (simple cycle) is marked on the bottom right of the figure. As illustrated in Figure 7(a), in order to keep TIT constant, fuel consumption (m_f) has to increase with ε_{eq} increasing and hence more fresh air (m_a) is required. Although reducing the pressure ratio of LPC (π_{LC}) and increasing the rotating speed of LPC (n_{LC}) can result in increasing of the air mass flow (m_a), neither n_{LC} nor m_a can increase infinitely because n_{LC} must be constrained by mechanical load and m_a by compressor characteristics. Keeping TIT = 1532 K, when ε_{eq} increases to 0.30, n_{LC} reaches its maximum 7700 r/min (given in Table 4). Then keeping n_{LC} = 7700 r/min, with increasing ε_{eq} further from the value of 0.30, the intercooled gas turbine still can work in certain extent (from 0.3 to 0.35) by reducing π_{LC} and increasing m_a, but the increasing of m_a becomes weaker and weaker until m_a cannot increase further because of the choke of LPC, while η_{LC} and η_{HC} drop in this process, leading to P_{GT} dropping. In addition, it can be seen in Figure 7(b) that the isolines of the efficiency of power turbine (η_{PT}) are approximately vertical with horizontal axis and lower obviously with n_{PT} decreasing, leading to P_{GT} dropping too. So the maximum power point (A) of the intercooled gas turbine is located on the upper right of Figure 7. Based on the above analysis, objective assessment to status A is given that the intercooler cannot perform fully in this case and the power enhancement of the intercooled gas turbine is not as remarkable as that of others with some components redesign.

We can find in Figure 7(b) that HPC subjects lower centrifugal stress due to the rotating speed of HPC (n_{HC}) reducing with ε_{eq} increasing. In addition, turbines subject lower thermal stress due to the cooling air temperatures reducing with ε_{eq} increasing. The only one disadvantageous effect on reliability of the intercooled gas turbine at status A is that about 3.4% overspeed of the low pressure shaft is required. And just for high TIT and n_{LC}, time limit must be considered when the intercooled gas turbine operates at this condition.

4.2.2. Maximum Continuous Power (Status B). As mentioned above, about 10% power enhancement of the intercooled gas turbine is realized by keeping TIT at 1532 K with 3.49% overspeed penalty of low pressure shaft, which brings time limit. So maximum power without time limit for ships to obtain maximum continuous cruising speed is another important

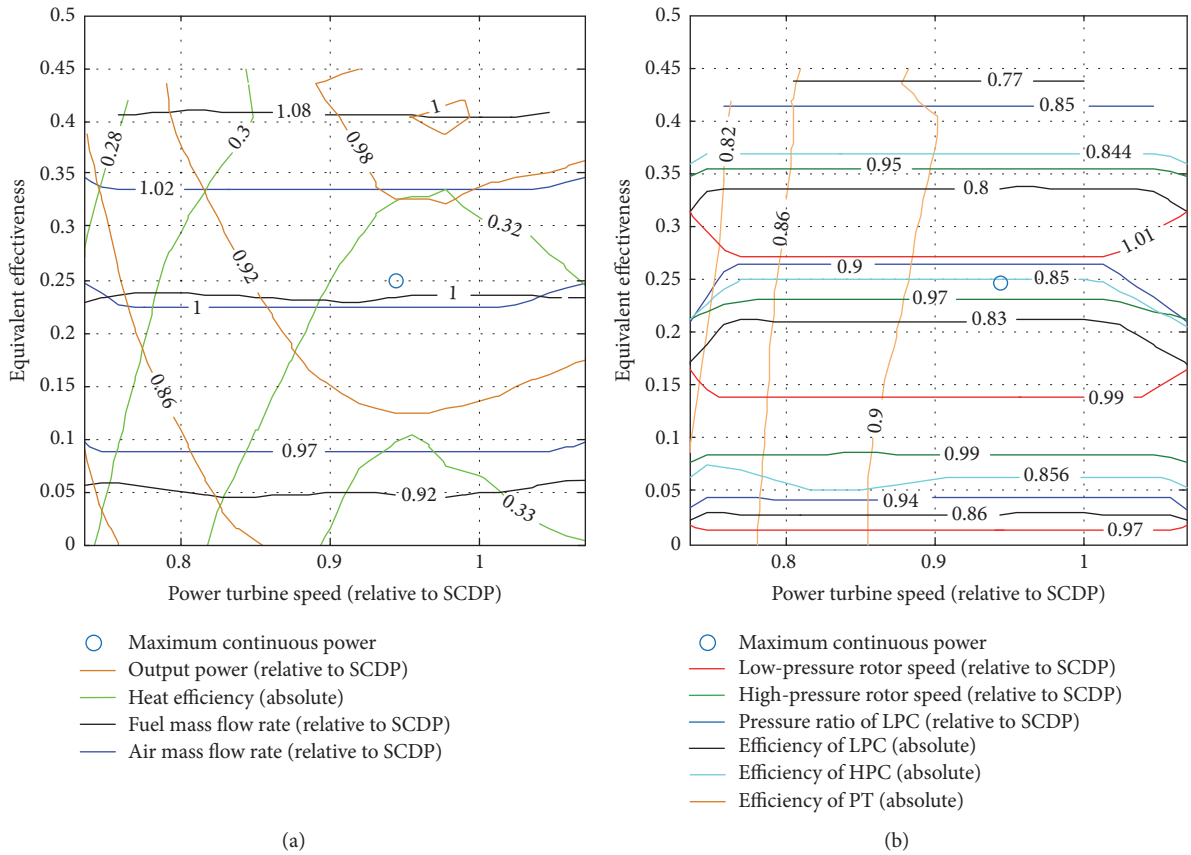

Figure 8: Meaningful parameters of intercooled gas turbine for TIT = 1481 K.

status that needs to be determined. For the purposes of extending system life, a slightly conservative assumption is made in this case that a TIT of 1481 K (the TIT level at 90% part-load of the existing gas turbine) acts as tolerable maximum value for continued operating of the intercooled gas turbine, while all the other operating parameters should be no longer permitted to exceed their values of the design point of the existing gas turbine too.

Figure 8 shows some meaningful parameters of intercooled gas turbine with constant TIT of 1481 K. Given the same values of n_{PT} and ε_{eq}, decreasing TIT from 1532 K (Figure 7) to 1481 K (Figure 8) brings some different behaviors as follows: P_{GT} decreases, as also can be observed in Figure 6 obviously that the isosurface of 1481 K locates under the isosurface of 1532 K; η_{GT} decrease as well; the tolerable operating range expands upward.

As can be seen in Figure 8(a), reducing only the parameter of ε_{eq} leads to lower P_{GT} and higher η_{GT}. So it is beneficial to carry out part-load by means of reducing ε_{eq} rather than by reducing TIT. In addition, it can be observed in Figure 8(a) that the peaks of power isolines and the bottoms of efficiency isolines have almost the same value of $\overline{n}_{PT}$ (about 0.95). Whether increasing or decreasing only the parameter of $\overline{n}_{PT}$ from the value of 0.95, the performance parameters of P_{GT} and η_{GT} drop. The aforementioned characteristic points (peaks and bottoms) with better performance form the local ridge of the isosurface of TIT (1481 K) in the three-dimensional space (Figure 6). Then the maximum power point without time limit (marked with letter B) is defined by the intersection of the local ridge and the isosurface of $\overline{n}_{LC} = 1$. Compared with 90% part-load of the existing gas turbine, the output power at status B (0.9427, 0.2483, and 0.9587) increases by 6.52% after adopting intercooling.

4.2.3. Operating Curve between Statuses A and B. Performance calculation indicated that points A and B have almost the same efficiency value (0.3249). The isosurface of η_{GT} (0.3249) has been drawn in Figure 6 and its local valley (marked with curve v) has been extracted on it. The local valley represents minimum fuel burn for the same power. It can be observed that points A and B lie nearby on the two sides of the local valley. On the other hand the same time limit is assumed at every power status above B by considering mechanical constraints and thermal constraints. Therefore the phase between A and B can be regarded as a pure transition which is not very important to be optimized at steady state conditions. So a simple and reasonable approach to obtain the operating curve of this transitional phase is to connect A and B along the shortest path on the isosurface of η_{GT} (0.3249).

4.2.4. Operating Curve below Status B. Figure 9 shows some meaningful parameters of intercooled gas turbine with constant TIT of 1350 K. Figure 9(a) shows that the peaks

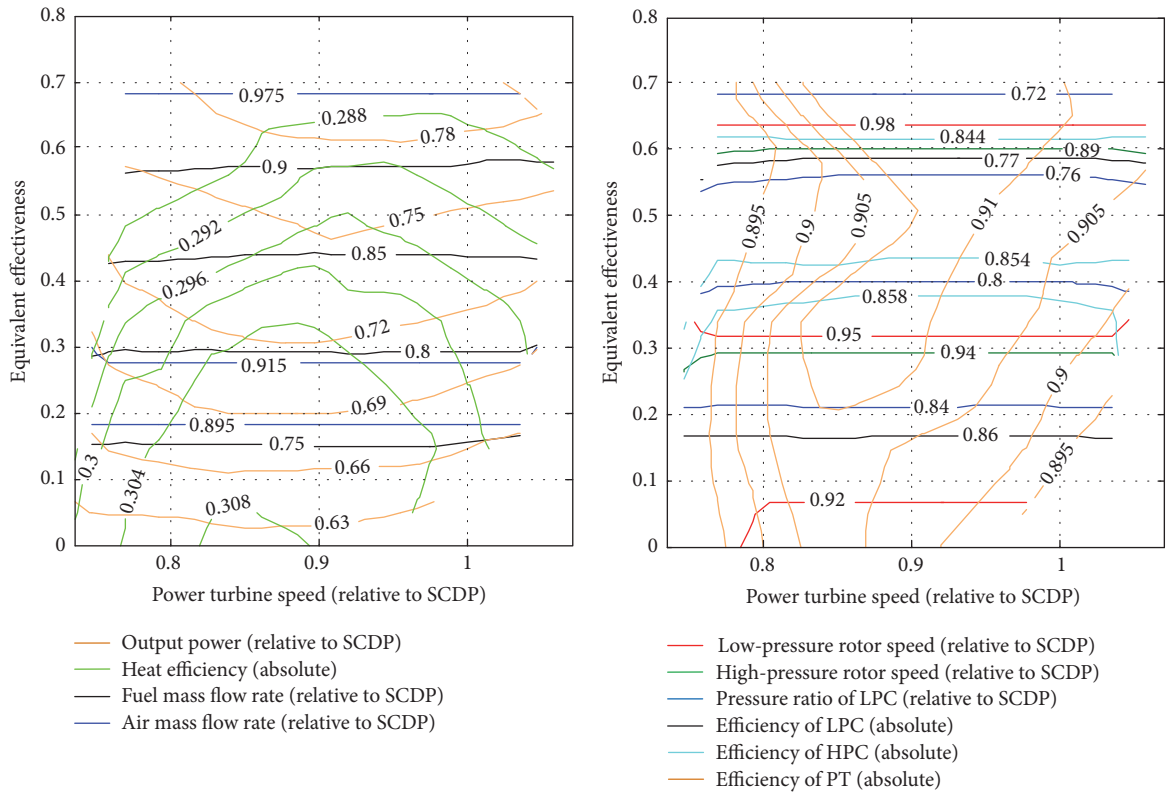

Figure 9: Meaningful parameters of intercooled gas turbine for TIT = 1350 K.

of power isolines and the bottoms of efficiency isolines move left at the same time by lowering ε_{eq}. Comparison of Figure 9 with Figures 7 and 8 shows that the improvement of P_{GT} by adopting intercooling becomes more notable with the decreasing of TIT. For example, P_{GT} can be enhanced more than 25% because n_{LC} is no longer being constrained (Figure 9(b)).

In this case heat efficiency of the intercooled cycle is always smaller than that of simple cycle at every TIT level (Figures 7–9). So the intercooler is not necessary to work when simple cycle can fulfill the output power. In the coordinate plane where ε_{eq} equals zero (Figure 6), an optimized operating curve (E-F) is obtained by conventional means of linking the bottoms of the isolines of η_{GT}. It intersects with the isosurface of TIT (1481 K) at point F (0.9975, 0, and 0.8780). On the other hand, based on aforementioned characteristics given to the local ridge on the isosurface of TIT (1481 K), the next operating curve below B will go along the ridge until arriving point C (0.9427, 0, and 0.8815) where ε_{eq} reduces to zero (Figure 6). The gap between points C and F brings at least three schemes to be chosen for appropriate operating curve below status B.

The first scheme (curve BFE) presented in Figure 6 is obtained by linking points B and F directly on the isosurface of TIT (1481 K). In doing so a vertical plane going through points B and F is used to intersect the isosurface of TIT (1481 K). The bottom half (EF) of the resulting curve (BFE) can keep optimal while the upper half (BF) loses a little efficiency. Besides, n_{PT} is unable to hold monotone.

The second scheme (curve BCFE) is obtained by linking points C and F. Both the upper section (BC) and the bottom section (EF) can keep optimized performance. Although the middle section (CF) also has satisfactory performance for its locating on isosurface of TIT (1481 K), a noticeable disadvantage is that n_{PT} cannot hold monotone too. Besides, it can be observed in Figure 6 that a slight change of P_{GT} (1%) in CF demands a violent change of n_{PT} (5%) correspondingly. Such an unusual local static amplification will arouse difficulty for controlling of the intercooled gas turbine.

The third scheme (curve BCDE) is obtained by using an auxiliary vertical line (CD) to replace the upper part of the curve EF, where D is the point of intersection of EF and the vertical line (CD) (seen in Figure 6). This method can keep better efficiency in the upper section (BC) and bottom section (DE) and can overcome the nonmonotone of n_{PT}. The defect of the method is that the efficiency drops in the middle section (CD). Based on the analysis above the third scheme is selected in this case as the operating curve below status B of the intercooled gas turbine in this case.

Thus, an appropriate operating curve (ABCDE) is defined in three-dimensional space for the intercooled gas turbine at the steady state, which covers the power range lasting from below 34% to above 109% of the design point of the existing gas turbine.

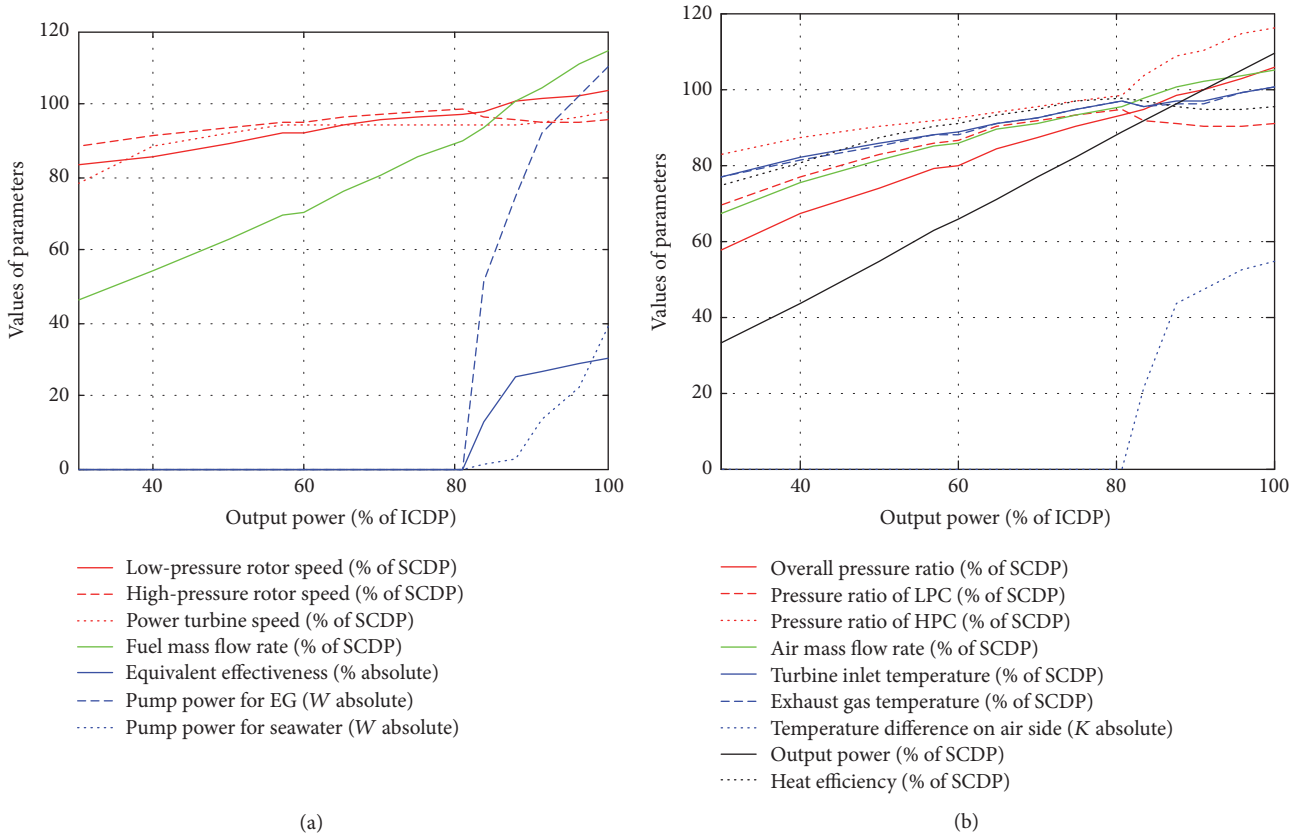

Figure 10: Values of some significant parameters on the optimal operating curve.

4.3. Control Strategy at the Steady State Conditions. Values of some consequential parameters of the intercooled gas turbine along the resulting operating curve (ABCDE) in the previous section are reported in Figure 10. These parameters are regarded as functions of dimensionless output power of the intercooled gas turbine. In doing so a 100% load of the intercooled cycle is defined at point A (109.1% load of the design point of simple cycle) and then every point on the operating curve can be represented by its corresponding percentage power value. After such a conversion the power range along the operating curve in Figure 10 lasts from 30% to 100%.

As can be seen in Figure 10, the optimized operating process of the intercooled gas turbine in this case is characterized by follows: (1) n_{PT} keeps as a constant in the power range from 60% to 90% part-load. (2) $\varepsilon_{\mathrm{eq}}$ keeps as zero in the power range below 80% part-load. (3) TIT keeps as a constant in the power range from 80% to 90% part-load. With these boundaries serving as demarcation points, a subdivision control strategy (being divided into 4 sections) can be adopted for the intercooled gas turbine in this case at the steady state conditions. Although the applying of $\varepsilon_{\mathrm{eq}}$ simplified the performance calculations and operating curve definition due to reducing the degrees of freedom by one, the on-engine intercooler and the off-engine intercooler need to be controlled, respectively, in practical running. So the section from 90% to 100% part-load is the most complex one in which four drive parameters are required simultaneously, that is, fuel mass flow rate (m_f), power consumption of pump for EG ($P_{P.\mathrm{EG}}$), power consumption of pump for seawater ($P_{P.s}$), and power turbine speed (n_{PT}, often being realized by pitch control). Comparatively speaking the section from 60% to 80% part-load is the simplest one with a single drive parameter of m_f while the other three parameters keep as constants. The numbers of drive parameters in the section from 30% to 60% part-load and the section from 80% to 90% part-load are two and three, respectively.

Along the operating range from 30% up to 80%, all parameters increase monotonically in order to enhance output power (P_{GT}). In contrast once the intercooler switch is at 80% part-load, the parameters of n_H and π_{LC} can no longer hold monotone in order to fulfill the matching among components, while P_{GT} continues increasing due to TIT and OPR and m_a increase monotonically. Thermal efficiency (η_{GT}) drops in the operating range from 80% to 100% because the line of m_f becomes more steep. It can be observed in Figure 10 that the maximum η_{GT} occurs at 80% part-load.

5. Conclusion

This work studied off-design performance calculation and operating curve design of marine intercooled gas turbine at steady state conditions. Major conclusions were drawn as follows:

(1) Regarding the defined equivalent effectiveness of an indirect fluid coupling intercooler as additional degree of freedom, taking the power consumption of pumps into account, a "decoupling-coupling" model of a marine intercooled gas turbine was developed for obtaining its off-design performance at steady state. Calculation results showed that the performance improvement of the intercooled gas turbine without any components redesigned was limited mainly by the inherent characteristic of the low pressure compressor. This limitation made the intercooler effectiveness be extravagant, which has been optimized based on the operating condition of a simple cycle gas turbine. The issues just indicate that certain conditions for optimizing often lead to uncertain optimization results. So it is necessary to think highly of the coupling between the intercooler and the existing gas turbine not only in operation curve optimization of an intercooled gas turbine but also in structural optimization of an intercooler. The coupling model developed in this study will be beneficial to the recommended integration optimization design in future research activities.

(2) With some geometric elements (peaks, ridges, or valleys on isosurfaces) revealing their potential for performance optimization, graphical method was applied to design the operating curve in three-dimensional space for an intercooled gas turbine at the steady state. Optimization results showed that the intercooling reforming (without any components redesigned) enhanced power level only by approximately 10% and even with some heat efficiency decreasing. This regret can be compensated to some extent by fewer reconstruction costs and superior reliability. Future investigations will deal with the performance optimization of an intercooled gas turbine with some new components by the graphical method proposed in this study to demonstrate its flexibility and workability further. The effect of intercooler effectiveness on the trade-off among output power, efficiency and lifetime will also be part of the investigation.

(3) For satisfying mechanical and thermal constraints as well as adapting typical sailing phase of ships, the control strategy of the intercooled gas turbine at steady state conditions was designed to subsection control, substantially being a kind of variable cycle control. According to the steeper trend of the fuel flow rate in the intercooling sections (Figure 10), one can infer that accidental shutdown of the intercooler will probably lead to overheat of turbines and overspeed of the high pressure shaft. So intercooling brings some problems about transient behaviors of the system and the work presented here can be expected to provide some reference for dynamic researching about marine intercooled gas turbine.

Notation

Acronyms

HPC: High pressure compressor
HPT: High pressure turbine
ICDP: Intercooled cycle design point
ICOP: Intercooled cycle operating point
LHV: Low heat value of fuel
LPC: Low pressure compressor
LPT: Low pressure turbine
OPR: Overall pressure ratio
PT: Power turbine
RGB: Reduction gearbox
SCDP: Simple cycle design point
TIT: Turbine inlet temperature

Variables

K: Overall heat transfer coefficient
m: Mass flow rate (kg/s)
n: Rotational speed (r/min)
P: Power (W)
p: Pressure (Pa)
T: Temperature (K)
Δp: Pressure drop (Pa)

Greek Symbols

ε: Heat exchanger effectiveness
η: Isentropic efficiency
η_m: Mechanical efficiency
π: Pressure ratio
Φ: Amount of heat

Subscripts

a: Air
cor: Corrected parameter
EG: Ethylene glycol
f: Fuel
GT: Gas turbine
g: Gas
H: High pressure shaft
HC: High pressure compressor
HT: High pressure turbine
in: Inlet section
L: Low pressure shaft
LC: Low pressure compressor
LT: Low pressure turbine
out: Outlet section
on: On-engine intercooler
off: Off-engine intercooler
P: Pump
PT: Power turbine
s: Seawater.

Conflicts of Interest

The authors declared that there are no conflicts of interest regarding the publication of this paper.

Acknowledgments

The present work is supported by the Fundamental Research Funds for the Central Universities of China (no. HEUCFM170301).

References

[1] K. G. Kyprianidis, T. Grönstedt, S. O. T. Ogaji, P. Pilidis, and R. Singh, "Assessment of future aero-engine designs with intercooled and intercooled recuperated cores," *Journal of Engineering for Gas Turbines and Power*, vol. 133, no. 1, Article ID 011701, 2011.

[2] N. Chandrasekaran and A. Guha, "Development and optimization of a sustainable turbofan aeroengine for improved performance and emissions," *Proceedings of the Institution of Mechanical Engineers, Part G: Journal of Aerospace Engineering*, vol. 227, no. 11, pp. 1701–1719, 2013.

[3] R. Bhargava, M. Bianchi, A. Peretto, and P. R. Spina, "A feasibility study of existing gas turbines for recuperated, intercooled, and reheat cycle," *Journal of Engineering for Gas Turbines and Power*, vol. 126, no. 3, pp. 531–544, 2004.

[4] X. Y. Wen and D. M. Xiao, "Feasibility study of an intercooled-cycle marine gas turbine," *Journal of Engineering for Gas Turbines and Power*, vol. 130, no. 2, Article ID 022201, 2008.

[5] X. Xiao, *The optimization design, modeling and control of the gas turbine intercooler [M.S. thesis]*, Shanghai Jiao Tong University, China, 2013.

[6] W. Dong, P. Gao, and P. Y. Zheng, "Optimal design and performance analysis of marine gas turbine intercooler," *Aeroengine*, vol. 37, no. 3, pp. 21–25, 2011.

[7] M. Kim, M. Y. Ha, J. K. Min, R. Stieger, A. Rolt, and C. Son, "Numerical study on the cross-corrugated primary surface heat exchanger having asymmetric cross-sectional profiles for advanced intercooled-cycle aero engines," *International Journal of Heat and Mass Transfer*, vol. 66, pp. 139–153, 2013.

[8] X. Zhao and T. Grönstedt, "Conceptual design of a two-pass cross-flow aeroengine intercooler," *Proceedings of the Institution of Mechanical Engineers, Part G: Journal of Aerospace Engineering*, vol. 229, no. 11, pp. 2006–2023, 2015.

[9] N.-B. Zhao, X.-Y. Wen, and S.-Y. Li, "Dynamic time-delay characteristics and structural optimization design of marine gas turbine intercooler," *Mathematical Problems in Engineering*, vol. 2014, Article ID 701843, 2014.

[10] D. H. Mallinson and W. G. Lewis, "The part-load performance of various gas-turbine engine schemes," *Proceedings of the Institution of Mechanical Engineers*, vol. 159, no. 1948, pp. 198–219, 1948.

[11] M. A. da Cunha Alves, H. F. de Franca Mendes Carneiro, J. R. Barbosa et al., "An insight on intercooling and reheat gas turbine cycles," *Proceedings of the Institution of Mechanical Engineers, Part A: Journal of Power & Energy*, vol. 215, no. A2, pp. 163–171, 2001.

[12] W. Wang, L. Chen, F. Sun, and C. Wu, "Power optimization of an irreversible closed intercooled regenerated brayton cycle coupled to variable-temperature heat reservoirs," *Applied Thermal Engineering*, vol. 25, no. 8-9, pp. 1097–1113, 2005.

[13] L. G. Chen, W. H. Wang, and F. R. Sun, "Ecological performance optimisation for an open-cycle ICR gas turbine power plant part 1: thermodynamic modelling," *Journal of the Energy Institute*, vol. 83, no. 4, pp. 235–241, 2010.

[14] W. H. Wang, L. G. Chen, and F. R. Sun, "Ecological performance optimisation for an open-cycle ICR gas turbine power plant part 2: optimisation," *Journal of the Energy Institute*, vol. 83, no. 4, pp. 242–248, 2010.

[15] W. H. Wang, L. G. Chen, and F. R. Sun, "Thermodynamic optimization of a triple-shaft open intercooled, recuperated gas turbine cycle. Part 1: description and modeling," *International Journal of Low-Carbon Technologies*, 2013.

[16] W. Wang, L. Chen, and F. Sun, "Thermodynamic optimization of a triple-shaft open intercooled, recuperated gas turbine cycle. Part 2: power and efficiency optimization," *International Journal of Low-Carbon Technologies*, vol. 11, no. 1, Article ID ctt054, pp. 29–34, 2014.

[17] H. Canière, A. Willockx, E. Dick, and M. De Paepe, "Raising cycle efficiency by intercooling in air-cooled gas turbines," *Applied Thermal Engineering*, vol. 26, no. 16, pp. 1780–1787, 2006.

[18] L. Xu and T. Grönstedt, "Design and analysis of an intercooled turbofan engine," *Journal of Engineering for Gas Turbines and Power*, vol. 132, no. 11, Article ID 114503, 2010.

[19] E. Najafi Saatlou, K. G. Kyprianidis, V. Sethi, A. O. Abu, and P. Pilidis, "On the trade-off between minimum fuel burn and maximum time between overhaul for an intercooled aeroengine," *Proceedings of the Institution of Mechanical Engineers, Part G: Journal of Aerospace Engineering*, vol. 228, no. 13, pp. 2424–2438, 2014.

[20] W. Camilleri, E. Anselmi, V. Sethi, P. Laskaridis, A. Rolt, and P. Cobas, "Performance characteristics and optimisation of a geared intercooled reversed flow core engine," *Proceedings of the Institution of Mechanical Engineers, Part G: Journal of Aerospace Engineering*, vol. 229, no. 2, pp. 269–279, 2015.

[21] W. Camilleri, E. Anselmi, V. Sethi et al., "Concept description and assessment of the main features of a geared intercooled reversed flow core engine," *Proceedings of the Institution of Mechanical Engineers, Part G: Journal of Aerospace Engineering*, vol. 229, no. 9, pp. 1631–1639, 2015.

[22] A. D. Rao and D. J. Francuz, "An evaluation of advanced combined cycles," *Applied Energy*, vol. 102, pp. 1178–1186, 2013.

[23] A. Kumari and Sanjay, "Investigation of parameters affecting exergy and emission performance of basic and intercooled gas turbine cycles," *Energy*, vol. 90, pp. 525–536, 2015.

[24] D. Cimini, J. A. Shaw, E. R. Westwater et al., "Air temperature profile and air/sea temperature difference measurements by infrared and microwave scanning radiometers," *Radio Science*, vol. 38, no. 3, pp. 10-1–10-19, 2003.

[25] A. Lin, J. Liang, D. Gu, and D. Wang, "On the relationship between convection intensity of South China Sea summer monsoon and air-sea temperature difference in the tropical oceans," *Acta Oceanologica Sinica*, vol. 23, no. 2, pp. 267–278, 2004.

[26] H. Choi and Y. H. Zhang, "Monthly variation of sea-air temperature differences in the Korean coast," *Journal of Oceanography*, vol. 61, no. 2, pp. 359–367, 2005.

[27] S. H. Wang, *Plate-FinHeat Exchanger*, Chemical Industry Press, Beijing, China, 1984.

[28] S. M. Jones, "Steady-state modeling of gas turbine engines using the Numerical Propulsion System Simulation code," in *Proceedings of ASME Turbo Expo 2010: Power for Land, Sea, and Air, GT 2010*, pp. 14–18, Glasgow, UK, 2010.

[29] C. J. Daniele, S. M. Krosel, J. R. Szuch, and E. J. Westerkamp, "Digital computerprogram for generating dynamic turbofan

engine models (DIGTEM)," NASA Technical Memorandum 83446, 1983.

[30] J. Y. Chen, *Calculation of component characteristics and overall advanced performance simulation of gas turbine [M.S. thesis]*, Harbin Engineering University, 2012.

[31] S. K. Zhang, *Simulation research on performance of marine intercooled cycle gas turbine [M.S. thesis]*, China Ship Research and Development Academy, 2012.

[32] B. H. Cheng and X. R. Li, "Plate heat-exchange device technical application manual," *China Building Industry Press*, 89, no. 68, 2005.